Ab initio Investigation of Pt Dimers on Cu(001) Surface

George Pal, Georgios Lefkidis,* and Wolfgang Hübner

Kaiserslautern University of Technology and Research Center OPTIMAS, P.O. Box 3049, 67653 Kaiserslautern, Germany

Received: May 4, 2009; Revised Manuscript Received: August 13, 2009

Using ab initio methods, we theoretically investigate the adsorption of one and two Pt dimers on Cu(001). Treating the interaction of adsorbates on surfaces as a local phenomenon, a representation of the substrate by a large cluster of at least 62 Cu atoms allows one to treat the electronic structures of both systems, that is, the adsorbate and the surface, on equal footing. Theoretical results concerning the adsorbate energetics, structure, and density of states are presented. We find that the Pt atoms of the adsorbates prefer to locate on top of the hollow sites of the Cu lattice. A symmetry-adapted-cluster expansion configuration-interaction method is used to calculate the excited states and the optical absorption spectra of the systems. The most intense peaks of the absorption spectra are around 1 eV and result from excited states of B_2 symmetry. Last but not least, we identify surface-mediated interdimer interactions.

Introduction

The adsorption of atoms and clusters at surfaces is the subject of intense ongoing investigation, both experimental and theoretical.[1−3] The reason for this is that the clusters have to be brought onto a surface or into an embedding medium in order to be of use in any technological application. It is well-known that the properties of clusters deposited on surfaces may significantly differ from those of the free species, opening a new field of building new materials with tailored properties. In this paper, we present real-space first-principles calculations, and we treat the adsorption of not only one but also two Pt_2 clusters on a nonmagnetic Cu(001) substrate. The molecular manipulation, stability, and dynamics of Pt dimers adsorbed on various surfaces have been the subject of several experimental investigations.[4−6] Here, we are mainly interested in the properties of the electronic system in the case of two Pt dimers deposited on Cu(001), which is a prototypical square-symmetric surface. This study will thus establish the Hilbert space necessary for further investigations such as the possibility of using surface plasmons as a means of transmitting information (e.g., a change in the electronic configuration induced by an applied laser field) from one adsorption site to the other. Therefore, a main part of the manuscript is dedicated to the calculation of the highly correlated electronic structure of the ground state and the energetically low-lying excited states. The excited states are necessary to determine the optical spectrum: the resonance energies of the optical absorption, where a coherent laser field excites electrons from occupied to unoccupied states, are given by the energy difference between the many-body ground state and the excited states, while the intensity of the lines are given by the oscillator strengths of the transitions between the initial and the final states.

An appropriate description of adsorption processes using first-principles approaches poses a serious challenge due to the distinct nature of the two systems, that is, the surface, which can be considered as a semi-infinite solid, and the adsorbate, which has a finite number of atoms. Two major schemes have been designed to theoretically address this problem. First, the slab and/or supercell method[7−9] is where one considers periodic units of a portion of the bulk plus the molecule, forming thus a fictitious periodic two- or three-dimensional lattice. Second, the cluster method,[1,2,10−12] treats the interaction between the adsorbates and the surfaces as a local phenomenon, so that the charge density changes only in the vicinity of the adsorbate. Therefore, this method attempts to provide an accurate description of the electrons in the region around the molecule and part of the substrate near it (the adsorbing region), while the rest of the surface, considered as a semi-infinite solid, does not feel the presence of the adsorbate. Last but not least, high-quality post-Hartree−Fock methods (like the SAC−CI used here) can only be applied in real-space, rendering the cluster model the only possible choice.

In both methods, it is reasonable to assume that coupling the adsorbate to as many unit cells from the substrate as possible leads to a more realistic description of adsorption. To mimic the two-dimensional character of the surface, the corresponding cluster is a fragment consisting of two or three layers cut out from the respective (semi)infinite ideal lattice. The distances between the atoms are usually kept at their bulk value, although some atoms in the adsorption region are allowed to relax in order to better describe the surface−adsorbate interaction.[13−15] One of the most important issues in this case is the convergence of the adsorption properties with respect to the cluster size. It is well-known that the calculated adsorption energies oscillate with the size and the shape of the cluster models.[16] This is because the surface electronic structure is represented insufficiently and also because a large fraction of substrate atoms lacks proper coordination. To obtain adsorption energies in reasonable agreement with experimental results, several strategies were proposed. One of them is based on the concept of bond preparation,[17,18] where a suitable excited state with proper energy and symmetry is used to interact with the adsorbate. However, the bond preparation is not generally applicable.[19,20] An alternative method to the cluster models with two-dimensional form is to use clusters with a thermodynamically stable octahedral or cuboctahedral shape in the case of nanocrystallites with face-centered cubic (fcc) structure.[21−23] For C

* To whom correspondence should be addressed. E-mail: lefkidis@physik.uni-kl.de.

10.1021/jp904133b CCC: $40.75
Published on Web 10/12/2009

and CO adsorbed on the (111) facets of large octahedral or cuboctahedral Pd clusters, it was shown that these three-dimensional cluster models yield a good cluster-size convergence of the adsorption properties.

Here, we are mainly interested in the properties reflecting the local character of the adsorbate−surface interaction. We concentrate our attention on the interaction mechanisms and the bond lengths, which only depend weakly on the cluster size. In the case of two Pt_2 adsorbed on Cu(001), the octahedral or cuboctahedral Cu cluster-approaches cannot be used, hence we consider a two-dimensional cluster model with three Cu layers. Also, we adopt a real-space wave function method, because we are interested in spatially resolved charge densities. Out of many possible soft landing scenarios, we choose the most favorable ones, and we calculate the dependence of the energy, the electronic structure, and the optical absorption spectrum of the systems on the distance between the Pt_2 clusters and the Cu surface. By analyzing the theoretical results, we are able to characterize the interactions between the adsorbates and the substrate and to identify the surface-mediated interactions among the dimers. The latter is important for technological applications since, in experimental setups, metallic substrates can alter the properties of the neighboring adsorbates, thus leading to new physics.

This manuscript is divided into three major parts. The first part is dedicated to results for the ground state of the cluster models employed to describe Pt dimers softly landing on the Cu(001) surface, and we discuss the geometry optimization and the electronic properties of the structures. In the second part, we elaborate on the interaction between the adsorbates and the surface with the help of a density of electronic states analysis. In the third part, we present results concerning the excited states and the optical absorption spectra of the systems, which are calculated using the symmetry-adapted-cluster configuration-interaction method.

Relaxation of Platinum Clusters on the Cu(001) Surface

In the case of adsorption at Cu surfaces, existing calculations estimate that using 14 to 38 Cu atoms is sufficient to get accurate results concerning the adsorption energies,[24−29] although calculations with up to 54 Cu atoms have been reported.[13] Here, we are not directly concerned with obtaining accurate results for the adsorption energy, but we interpret them as a qualitative guide when it comes to choosing between different landing scenarios. In the case of one Pt dimer adsorbed on Cu(001), we model the surface with a cluster comprising of 5×6, 4×5, and 3×4 Cu atoms in the first, second, and third layer, respectively, as can be seen from panel A of Figure 1. With this choice, we take into account surface Cu atoms which are neighbors of first, second, and third order with the Pt atoms of the adsorbates. In the case of two Pt dimers adsorbed on a Cu surface, we use a larger Cu cluster, depicted in panel B of Figure 1 and comprising of 5×7, 4×6, and 3×5 atoms in the first, second, and third layer, respectively. The geometry optimization of the structures is performed for the ground state using the density functional theory (DFT) as implemented in the Gaussian 03 quantum chemistry package.[30] In our DFT calculations, we use the B3LYP hybrid functional, where the exchange interaction is given by the Becke functional[31] which includes the Slater exchange together with corrections involving the gradient of the density, and the correlation term is given by the Lee, Yang and Parr functional,[32] which includes both local and nonlocal contributions.

To find the equilibrium configuration of the ground state, only the distance d_{Pt-Pt} between the Pt atoms is optimized for different values of the distance h_{Pt} between the surface and the Pt dimer. The Pt atoms are fully relaxed with the constraint of the C_{2v} symmetry. To further simplify the calculations, we use two different basis sets and effective core-potentials for the Cu atoms, depending on their positions with respect to the Pt atoms. So, Cu atoms right under the Pt dimers and from the first and second layer are represented by the double-ζ basis functions in the (5s5p5d)/[3s3p3d] configuration and Los Alamos effective core potentials (ECP) LANL2DZ,[33] while the rest of the Cu atoms are represented by the basis functions in the (4s5d)/[1s1d] configuration and the shape-consistent average relativistic ECPs.[34] For the Pt atoms, we use the LANL2DZ basis functions in the (5s6p3d)/[3s3p2d] configuration.

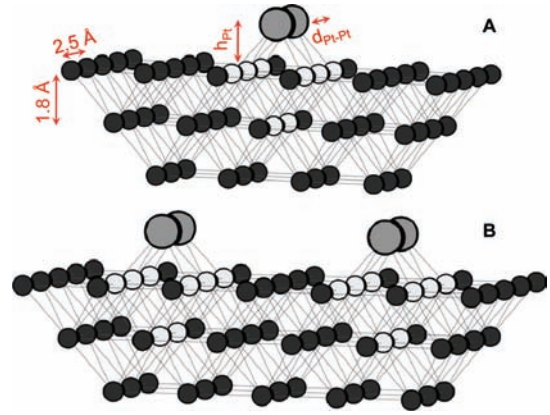

Figure 1. Adsorption of one (panel A) and two (panel B) Pt dimers on the Cu(001) surface represented by 62 (A) and 74 (B) Cu atoms. The highlighted Cu atoms are characterized by a larger basis set and a smaller ECP describing 10 electrons, while the peripheral Cu atoms have a smaller basis set and a larger ECP that in addition includes 3s and 3p electrons (see text).

We first discuss the case of a single Pt_2 cluster. The model depicted in panel A of Figure 1 is obviously not the only way of adsorption of Pt_2 on Cu(001). The interaction between the Pt atoms of the landing cluster and the Cu atoms of the surface can lead to a large number of possible equilibrium configurations. To study different landing scenarios, we consider six cases for the cluster models, which are chosen on symmetry grounds, namely, the two Pt atoms from the dimer are always kept in identical surroundings on the surface. The geometry optimization is performed in such a way that each Pt atom is coordinated with the same configuration of Cu atoms from the surface and the respective C_{2v} and C_2 symmetry is preserved. The six adsorption cases schematically shown in the upper panel of Figure 2 correspond to the initial configuration, that is, before performing the geometry optimization of the structures. The names of the different adsorption possibilities used here correspond to the following configurations: aligned-hollow (Model 1), aligned-atop (Model 2), aligned-bridge (Model 3), diagonal-hollow (Model 4), cross-bridge (Model 5), and diagonal-atop (Model 6).

Note that in order to preserve the symmetry and to have even numbers of Cu atoms for closed-shell calculations, the truncated-pyramid shape for the Cu cluster has to be different for each case. Using the same Cu cluster for each landing scenario leads to considering systems with nondefined symmetries. Denoting by $m \times n$ the number of Cu atoms in the upper layer (in each subsequent layer m and n are decreased by 1), we use $m = 5$ and $n = 6$ for Models 1 and 2 (62 Cu atoms), $m = 5$ and $n = 5$ for Models 3 and 4 (50 Cu), and $m = 4$ and $n = 6$ for Models 5 and 6 (50 Cu). Consequently, the number of Cu atoms near the Pt_2 cluster having a larger basis set is different for each

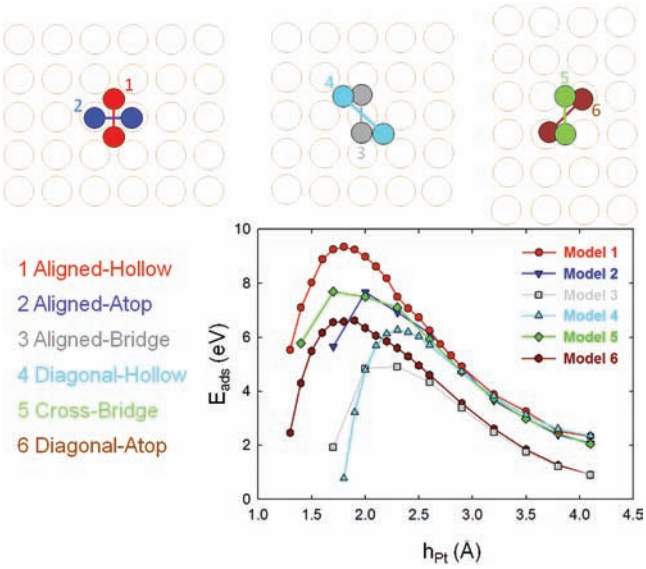

Figure 2. Upper panel: schematic top view of the six cluster models used to study the adsorption of one Pt dimer on Cu(001). Lower panel: Calculated adsorption energies for the $Pt_2Cu_{50/62}$ system as a function of the distance between the dimer and the surface. The most favorable geometry configurations correspond to larger adsorption energies.

model. Model 1 (aligned-hollow) corresponds to the situation shown in Figure 1.

The geometry optimization is performed for each model in order to find the equilibrium d_{Pt-Pt} distance for several values of the h_{Pt} parameter. Because one cannot directly compare the total ground-state energies of the optimized structures, we compare the adsorption energies, which are calculated according to the equation

$$E_{ads} = -(E_{Pt_2 \oplus Cu(001)} - E_{Pt_2} - E_{Cu(001)}) \qquad (1)$$

Here, $E_{Pt_2 \oplus Cu(001)}$ is the total energy of the substrate plus adsorbate system, E_{Pt_2} is the energy of the free dimer, and $E_{Cu(001)}$ is the total energy of the bare Cu cluster. Because of the minus sign in the right-hand side of eq 1 for the adsorption energy, a positive E_{ads} means that the total ground state energy of the adsorbed cluster with the surface is lower than the sum of the total energies of the separate cluster and of the substrate. Therefore, a larger adsorption energy corresponds to a more stable landing configuration. The lower panel of Figure 2 shows the adsorption energies of the geometry optimized $Pt_2Cu_{50/62}$ structures as a function of the h_{Pt} parameter. From the adsorption energy point of view, the most favorable landing scenario is when the Pt atoms are above the hollow sites of the upper Cu layer corresponding to Model 1, with an adsorption height of 1.794 Å. For this value of h_{Pt}, the distance between the Pt atoms is $d_{Pt-Pt} = 2.77$ Å. To ensure that the distances d_{Pt-Pt} and h_{Pt} converge with the number of layers, we have performed additional calculations for the Model 1 (aligned-hollow) starting from 62 Cu atoms (30 in the first, 20 in the second, and 12 in the third layer) and subsequently adding Cu atoms in the third and in the fourth layer with the constraint of preserving the overall C_{2v} symmetry. Thus, we consider large Cu clusters (of up to 100 atoms) for the substrate containing 3×4, 3×6, 5×4, and 5×6 atoms on the third and 2×1, 2×3, 2×5, 4×1, 4×3, and 4×5 atoms on the fourth layer. At the end of the geometry optimization, we obtain values $d_{Pt-Pt} = 2.772$ (±2.142%) Å and $h_{Pt} = 1.794$ (±2.006%) Å, which is a confirmation that considering three layers is enough for the calculations. In the case of Models 2, 3, and 4, the geometry optimization yields a distance between the Pt atoms of more than 5.1 Å (not shown) which is larger than twice the Cu−Cu distance when the Pt dimer is close to the surface ($h_{Pt} < 1.8$ Å). That means that the Pt_2 clusters dissociate when landing on the surface, and the Pt atoms prefer to locate themselves on top of the hollow sites of the Cu(001) substrate. This is in agreement with helium scattering experiments which yield the adsorption potential energy surface of sodium adatoms on Cu(001), characterized by a deep minimum at the hollow sites and a less pronounced minimum at the on-top sites.[35]

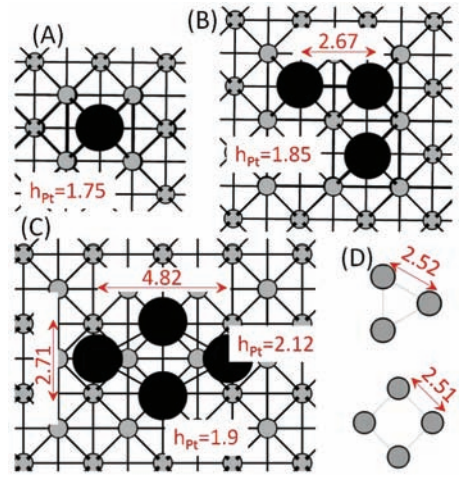

Figure 3. Most stable configurations of Pt, Pt_3, and Pt_4 on Cu(001). Distances are in angstroms. The geometries of the free clusters are also shown.

As mentioned above, for Pt_2 on Cu(001) the most favorable form of adsorption is when the Pt atoms are above the 4-fold hollow sites of the Cu lattice, corresponding to Model 1. Of course, this is not a general rule for the preferred form of adsorption of dimers. Many experimental and theoretical investigations have shown that, depending on the nature of the ad-dimers and of the substrate, the ad-dimers have different orientations with respect to the atoms from the substrate. However, for most of the systems (and we mention here V_2 on Cu(001),[27] Si_2 on Si(100),[36] SnGe on Ge(001),[37] Au_2Cu_2 and AuCu on Au(110),[38] Si_2 on Ge(100),[39] Sb_2 on Si(001)[40]), the dimers are parallel to the surface. A remarkable exception is the CO molecule on Cu(001) surface, which is oriented perpendicular to the surface and located above the Cu atoms.[41] We have also performed geometry optimization calculations for the case when the Pt_2 cluster is placed perpendicular to the surface, for three situations: above the Cu atoms, above the 4-fold hollow and the bridge sites of the Cu lattice. The results show that the Pt_2 perpendicular to the Cu(001) configuration is energetically less favorable than the parallel configuration. Pt_2 parallel to Pt and Ge surfaces has been observed in scanning tunneling microscopy experiments.[4−6]

We also study the size effect of a Pt cluster landing on the Cu surface. To this end, we have calculated the adsorption properties of Pt, Pt_3, and Pt_4, in addition to the Pt_2 cluster on the Cu(001). For the surface, the same three Cu clusters are employed, like in the case of Models 1−6 of adsorption for Pt_2 (see Figure 2). We find that the Pt adatom prefers to be situated above the 4-fold hollow sites of the Cu lattice, with an adsorption height of 1.75 Å; see panel A of Figure 3. When the Pt atom is placed above the bridge site, then the adsorption height is 2.03 Å and an extra energy of 0.4 eV is necessary.

The most unfavorable situation is when the Pt atom is placed above a Cu atom from the surface: an extra energy of 2.02 eV needs to be invested and $h_{Pt} = 2.34$ Å.

The free Pt_3 cluster has the equilibrium geometry of an equilateral triangle, with the side of 2.52 Å, in agreement with ref 42. This value is 0.6 Å smaller than the value obtained with a restricted Hartree−Fock geometry optimization.[43] The linear Pt_3 cluster has an energy of 1.9 eV higher than the total ground-state energy of the triangular cluster and therefore is energetically less favorable. When Pt_3 lands on the Cu(001) surface, the shape of the adsorbed cluster is not an equilateral triangle any more: the Pt atoms prefer to locate above the 4-fold hollow sites of the substrate; see panel B of Figure 3. Other configurations are energetically unfavorable, with an energy difference of up to 0.2 eV with respect to the energy of the equilibrium geometry.

For the free Pt_4, the square-planar geometry has the lowest energy with the square side of 2.51 Å, in agreement with ref 42. The optimized trigonal-pyramid structure with C_{3v} that we have also considered has a total ground state energy of 0.55 eV higher than the square planar cluster, therefore less energetically favorable. When Pt_4 is adsorbed on Cu(001), then the most stable configuration is obtained when two of the Pt atoms are above the 4-fold hollow sites and two Pt atoms are above the bridge sites of the Cu lattice, with different adsorption heights; see panel C of Figure 3. Other configurations need extra energy in order to be realized. For example, when the Pt atoms are above the 4-fold hollow sites of the Cu lattice, then the adsorption energy is 2.91 eV lower than the equilibrium energy (lower adsorption energy means an energetically less favorable configuration, due to the minus sign in the RHS of eq 1).

To determine the most suitable Pt cluster to be adsorbed on Cu(001), we compare the adsorption energy corresponding to a single Pt atom according to $E_{Pt} = -(E_{Pt_n \oplus Cu(001)} - E_{Cu(001)})/n$, where n is the number of Pt atoms in the cluster. We find that E_{Pt} is maximum for Pt_2 on Cu(001), and this corresponds to the most suitable cluster. For the Pt adatom, this energy is 0.2 eV lower, while for Pt_3 and Pt_4, this value is 0.6 and 0.76 eV lower, respectively.

The landing of two Pt dimers on Cu(001) within Model 1 (aligned-hollow) of adsorption reveals similar relaxation mechanisms as in the case of a single Pt dimer. In both cases, when the Pt dimers are far away from the surface ($h_{Pt} > 10$ Å), we obtain for d_{Pt-Pt} the correct free Pt_2 result, which is 2.34 Å.[44] As the Pt_2 clusters approach the surface, the distance between the Pt atoms does not become commensurate with the Cu lattice constant but instead takes values larger than 2.556 Å, as can be seen in the top panel of Figure 4. As in the case of one Pt dimer, the minimum-energy configuration for two Pt dimers occurs when the distance between the Pt and the surface is 1.8 Å. Note that for Pt_2Cu_{62} the geometry optimization at $h_{Pt} = 2.5$ and 2.6 Å leads to values of the d_{Pt-Pt} parameter which are larger than expected, and the corresponding curve is not smooth in this region but suffers instead a sudden jump. This situation corresponds to a crossing of the total energies of the optimized structures with the total energies of the structures corresponding to values of d_{Pt-Pt} which would make the curve smooth but have higher total energies.

We have also considered three Pt_2 on Cu(001), within Model 1 of adsorption. The distance between the parallel clusters is taken to be 5.11 Å, which is twice the Cu lattice constant. Calculations for several large Cu clusters were performed, with three layers and containing 44, 62, 86, and 110 atoms (8×3, 6×5, 8×5, and 10×5 Cu atoms in the upper layer,

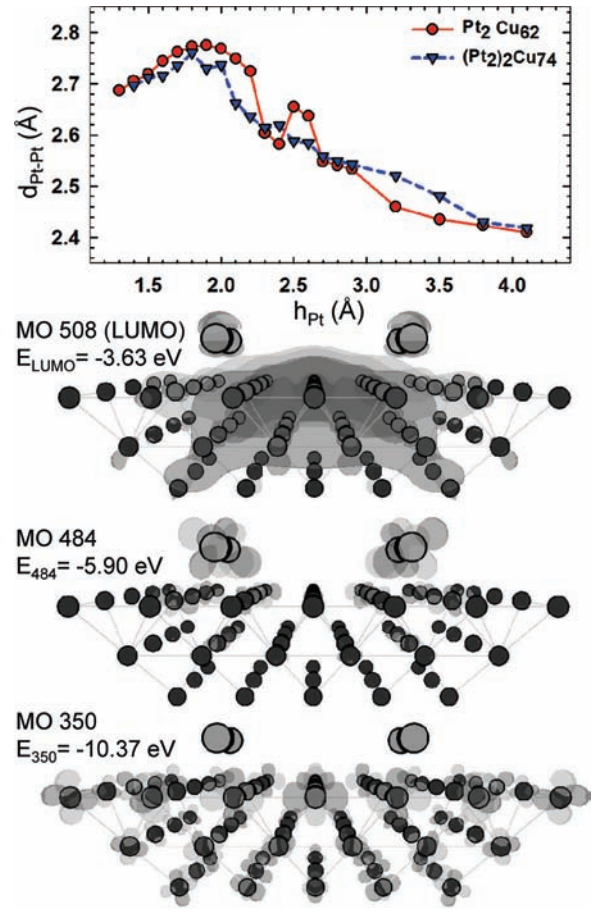

Figure 4. Top panel: the relaxation of one (circles) and two (triangles) Pt dimers landing on Cu(001). Bottom panels: three MOs of the $(Pt_2)_2Cu_{74}$ structure, presented by isosurfaces.

respectively). For all of the clusters, the geometrical parameters $d_{Pt-Pt} = 2.75 \pm 0.02$ Å and $h_{Pt} = 1.8 \pm 0.02$ Å agree well with the results obtained in the case of one and two Pt_2 on Cu(001).

According to the Mulliken population analysis, charge gets transferred from the Cu atoms of the surface to the Pt atoms of the adsorbates. This is substantiated by the fact that, for the Cu_{62} and Cu_{74} structures alone (i.e., without the Pt dimers), the highest occupied molecular orbitals (HOMO) are situated at −3.98 and −4.34 eV, respectively, which are higher than the lowest unoccupied molecular orbitals (LUMO) of the free Pt_2 and $(Pt_2)_2$ clusters (i.e., without the Cu substrate), which lie at −4.92 and −4.93 eV, respectively. When the two separate systems are brought together and after the equilibrium is established, electrons from the occupied states in the vicinity of the HOMO of the Cu surface are transferred to empty states in the vicinity of the LUMO of the Pt clusters.

Concerning the shape of the single-particle wave functions yielded by our real-space calculations, we can distinguish between three main types of molecular orbitals (MO). The bottom panels of Figure 4 show three MOs of the $(Pt_2)_2Cu_{74}$ cluster, which are relevant when one qualitatively discusses the interaction between the Pt dimers and the Cu surface. For MO 484, the main contribution to the wave function comes from the Pt dimers, while the contribution from the Cu atoms is small. On the contrary, for MO 350, the wave function is localized around the Cu atoms, and the quasi-periodicity of the isosurface with respect to the lattice constant resembles the Bloch functions specific to an infinite system. In the case of MO 508, which is also the LUMO, the wave function is spread throughout the

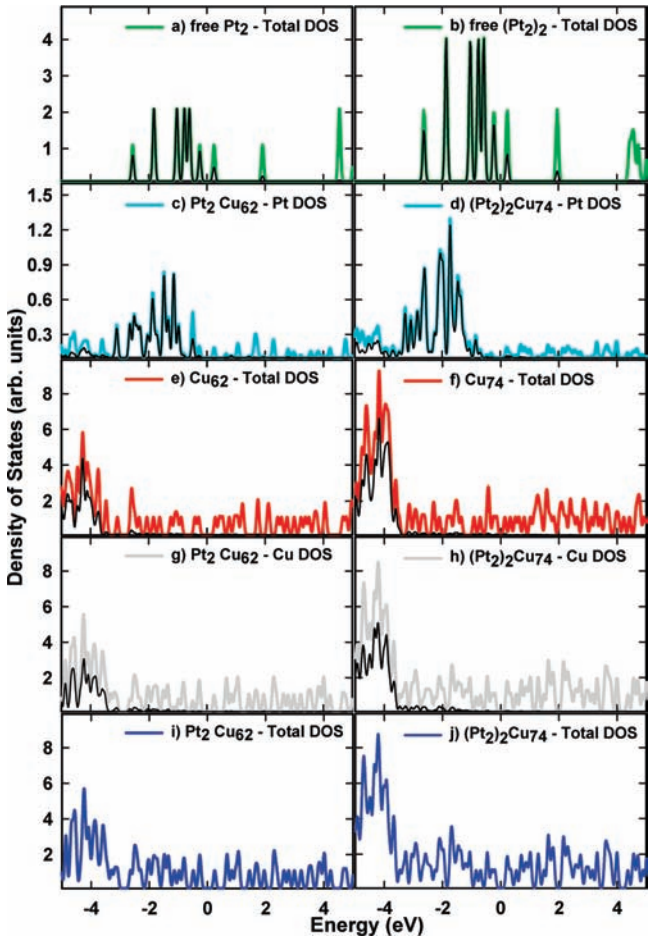

Figure 5. (a,b) DOS of one and two free Pt_2 clusters; (c,d) projected DOS of the Pt dimers in the presence of the respective substrate; (e,f) DOS for the Cu surfaces calculated without the adsorbate Pt dimers; (g,h) projected DOS of the Cu surfaces in the presence of the Pt dimers; (i,j) Total DOS of the Pt_2Cu_{62} and $(Pt_2)_2Cu_{74}$ structures. Negative and positive energies separate occupied from unoccupied states. The single-particle states have been broadened by 0.5 eV. Arbitrary units are used, but the scales are the same for each pair of panels. For c, d, and g−j panels, $h_{Pt} = 1.8$ Å. In panels a−h, the projected DOS corresponding to the d orbitals of Cu and Pt is highlighted by the black lines.

whole system, with contributions from both the adsorbates and the substrate, and one deals in this case with surface-mediated interactions between the adsorbates.

Electronic Density of States

To describe the nature of the interaction between the adsorbates and the substrates, we analyze in the following the electronic density of states (DOS) yielded by the DFT calculation. Figure 5 shows the total DOS and the projected DOS of the surfaces and of the adsorbates atoms of the Pt_2Cu_{62} and $(Pt_2)_2Cu_{74}$ structures, with $h_{Pt} = 1.8$ Å, as well as the DOS for the free Pt and Cu clusters. In the case of Pt_2Cu_{62} ($(Pt_2)_2Cu_{74}$), the DFT calculation involves 544 (788) MOs, and the eigenvalue spectrum stretches over a wide energy range, from $E_1^{MO} = -118.8$ eV ($E_1^{MO} = -118.0$ eV) to $E_{544}^{MO} = 415.5$ eV ($E_{788}^{MO} = 662.6$ eV). For clarity, in Figure 5, we restrict ourselves to the energy region in the vicinity of the HOMO and the LUMO, and the energy scale is adjusted so that zero energy corresponds to the middle of the HOMO−LUMO gap. For the adjusted energy scale, negative and positive energies separate occupied from unoccupied states. Comparing the total and the projected DOS from panels c,d,g−j, it is clear that the HOMO (in absolute values, $E_{HOMO}^{MO} = -4.47$ and -4.04 eV for Pt_2Cu_{62} and $(Pt_2)_2Cu_{74}$, respectively) and the LUMO ($E_{LUMO}^{MO} = -3.97$ and -3.63 eV) are associated with the substrate Cu atoms. The states from -3.5 to -0.5 eV below the HOMO have a strong influence from the Pt atoms, while the DOS above the LUMO is mainly influenced by the surface.

The presence of the surface drastically influences the DOS of the Pt dimers, as can be seen in panels a−d of Figure 5. For the DOS of two Pt_2 clusters from panel b, the distance between the Pt dimers is such that the direct interaction among them is minimal, a fact that proves that the selection of the distance between the two dimers is large enough. Compared with the results for the free Pt dimers shown in panels a,b, the projected DOS corresponding to the Pt dimers adsorbed on Cu(001) from panels c,d has a denser structure for Pt_2 on Cu_{62} and an even denser one for two Pt_2 on Cu_{74}. This is because the electronic properties of the Pt dimers combine now features of finite as well as extended systems. In panels c,d and in the energy interval from -3.3 to -0.8 eV, the DOS is associated with the d electrons of Pt, while the last two occupied states, as well as the unoccupied states that lie energetically close to the LUMO are associated to the s and p electrons of Pt, for both the Pt_2Cu_{62} and $(Pt_2)_2Cu_{74}$ structures. The peaks of the DOS of Pt in the $(Pt_2)_2Cu_{74}$ are denser and higher than those corresponding to Pt_2Cu_{62} because more Pt atoms and therefore more MOs are taken into consideration. The presence of the adsorbates influences also the properties of the substrate. In comparing the DOS of the surfaces (panels e,f of Figure 5) with the projected DOS corresponding to the substrate Cu atoms in the presence of the Pt dimers (panels g,h of Figure 5), there are noticeable differences regarding the position and the shapes of the peaks, which are shifted by up to 0.05 eV when Pt dimers are adsorbed on the substrate. There are still some common features, such as the main peak structures in the -5.0 to -3.6 eV energy interval, which have a strong d character, while the rest of the peaks result from s- and p-like states.

Analyzing the shape of each MO, one can distinguish between several contributions to the individual peaks of the DOS corresponding to the respective MO eigenvalue. For example, the MO 484 of the $(Pt_2)_2Cu_{74}$ cluster shown in Figure 4 is situated at -2.07 eV below the Fermi level (taken in the center of the HOMO−LUMO energy gap). As previously discussed, the main contribution to this MO comes from the Pt dimers and has a pronounced d-like character, while the contribution from the Cu surface is small. By examining now the DOS of $(Pt_2)_2Cu_{74}$ from Figure 5, the peak at -2.07 eV of the total DOS (panel j) comes mainly from the projected DOS of the Pt dimers (panel d) with a pronounced d-like character, which is small in the case of the projected DOS of the Cu atoms from the surface (panel h) and is nonexistent for the DOS of the Cu_{74} cluster (panel f). Another example is the first peak in the total DOS above zero energy, which corresponds to the LUMO. The main contribution to this peak comes from the projected DOS of the Cu atoms from the surface, but there is also some small nonzero contribution from the projected DOS of the Pt dimers. This can also be seen from the shape of the LUMO as depicted in Figure 4: the orbital is spread throughout the whole structure, mainly in the region of the Cu surface and with some contribution localized around the Pt dimers.

Excited States and Optical Absorption Spectra

In the following, we present results for the excited states of the systems, calculated using the symmetry-adapted-cluster configuration interaction (SAC−CI) method.[45−47] In SAC−CI,

which is a post-Hartree−Fock method, the wave function of the ground state is given by the SAC expansion

$$\Psi_g^{\mathrm{SAC}} = \mathscr{P}\left(\sum_I C_I S_I^\dagger\right)|0\rangle \tag{2}$$

where $|0\rangle$ is a single Hartree−Fock determinant, $S_I^\dagger$ is a symmetry-adapted excitation operator, and $\mathscr{P}$ is a symmetry operator. The SAC−CI wave function of the excited state is constructed by applying the symmetry-adapted excitation operator $\mathscr{R}$ to the SAC ground-state wave function

$$\Psi_e^{\mathrm{SAC-CI}} = \mathscr{R}\Psi_g^{\mathrm{SAC}} \tag{3}$$

In our calculations, the $\mathscr{R}$ operators are restricted to single and double excitations, and the excited states are singlets. The SAC−CI excited states are computed for the cluster structures given by the ground-state geometry optimization.

We discuss here the results for the excited states of the $(Pt_2)_2Cu_{74}$ cluster. Out of the 788 MOs used in the ground-state calculations, we select MOs from 489 to 534 for the active space for the correlated calculations. Thus, the active space comprises of 38 electrons distributed over 46 MOs. The window was chosen in such a manner that the energies of the lowest occupied and of the highest unoccupied MOs of the window are centered with respect to the Fermi level. In this way, all single-particle excitations with an energy of 0.15 eV are included, both from the HOMO and from the lowest unoccupied MO of the window. The 20 lowest-energy optically active excited states are computed for each of the four irreducible representations of the C_{2v} point group (i.e., A_1, A_2, B_1, and B_2).

We refer in the following to the optical absorption spectra of the $(Pt_2)_2Cu_{74}$ cluster, calculated from the excitation energies and the respective oscillator strengths. The oscillator strengths are given by the equation

$$f_{12} = \frac{2}{3}\frac{m_e}{\hbar}(E_2 - E_1)\left|\langle\Psi_1|\mathbf{R}|\Psi_2\rangle\right|^2 \tag{4}$$

where m_e is the electron mass, E_1 is the energy of the initial state Ψ_1, E_2 is the energy of the excited state Ψ_2, and $\mathbf{R}$ is the sum of the coordinates of all N electrons in the system, i.e., $\mathbf{R} = \sum_{i=1}^{N}\mathbf{r}_i$. The position of the resonance lines of the optical absorption spectrum, that is, the power spectrum, are given by the difference between the total energy of the many-body ground state and the energies of the excited states, and the intensities of the lines are determined by the oscillator strengths. We have considered two cases for Ψ_1 from which the excitations occur: first the SAC ground state $\Psi_1 = \Psi_g^{\mathrm{SAC}}$, which has A_1 symmetry, and second the lowest-energy SAC−CI state with A_2 symmetry $\Psi_1 = \Psi_{1(A_2)}^{\mathrm{SAC-CI}}$. Considering different symmetries of the initial state allows one to investigate different selection rules as well as the effect of the polarization of the light on the absorption spectra peaks. In our case, the transitions $A_1 \leftrightarrow A_1$ and $A_2 \leftrightarrow A_2$ require polarization of the incident light perpendicular to the surface, while for the transitions $A_1 \leftrightarrow B_1$, $A_1 \leftrightarrow B_2$, $A_2 \leftrightarrow B_1$, and $A_2 \leftrightarrow B_2$, field polarization parallel to the surface is needed.

The results for the first case are presented in Figure 6 with different values of the h_{Pt} parameter. The curves are obtained by applying Gaussian broadening with full width at half-maximum of 0.05 eV of the resonance lines. Because excitations are from the SAC ground state which has A_1 symmetry and the transitions $A_1 \leftrightarrow A_2$ are forbidden by the electric-dipole selection rules, the corresponding oscillator strengths are zero. The shape, peak positions, and widths of the absorption spectra change as the Pt_2 clusters approach the surface. However, there are certain common features: For all values of h_{Pt} considered, most of the optical absorption takes place in the energy interval from 0.5 to 2.0 eV. As a general trend of the absorption spectra, the intense peak is blue-shifted from 0.96 eV for $h_{Pt} = 1.7$ Å to 1.11 eV for $h_{Pt} = 3.2$ Å and its height decreases. Simultaneously, the structures corresponding to the energy interval from 1.5 to 2.2 eV are slightly red-shifted and the peaks are energetically reordered. The excited states with A_1 symmetry are important only when the Pt adsorbates are close to the surface, and their most prominent peaks are those around 1.36 eV. For all of the spectra, the highest peaks are due to excitations from the SAC ground state to the excited states with symmetry B_2, corresponding to a polarization change along the axis that unites the two Pt_2 adsorbates (by convention the O_y axis). We interpret this as a signature of intra-adsorbate transitions which are mediated by the underlying surface. The $A_1 \leftrightarrow B_1$ transitions, having a smaller contribution to the absorption spectra, are oriented along the Pt−Pt axis (O_x). The smallest contribution is given by the $A_1 \leftrightarrow A_1$ transitions, which are oriented perpendicular to the surface (i.e., along the O_z axis).

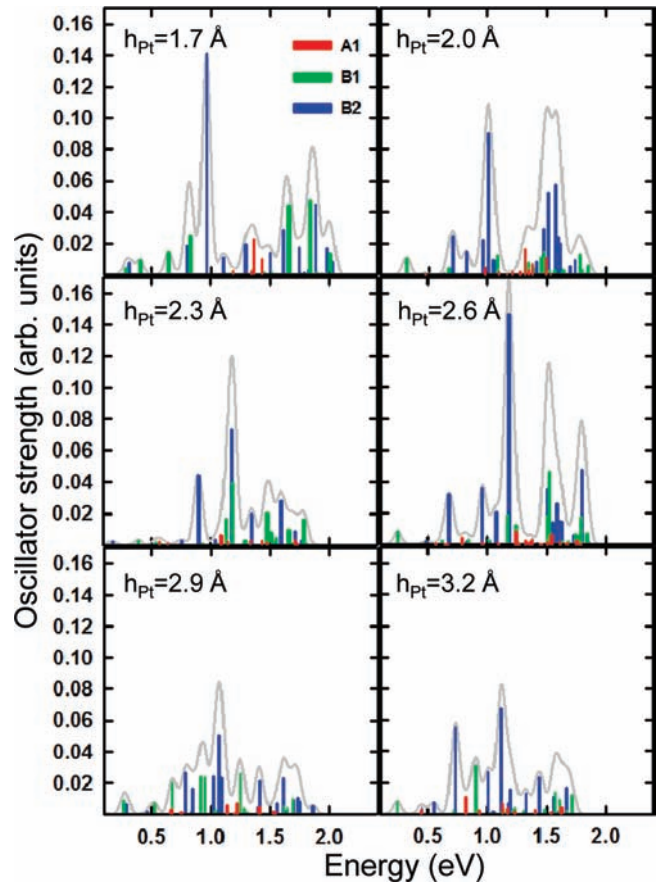

Figure 6. Excitation energies and the oscillator strengths (arbitrary units) of the $(Pt_2)_2Cu_{74}$ structure for several values of the h_{Pt} parameter indicated in Å. The initial state of the excitation is the SAC ground state, which has A_1 symmetry.

Figure 7 shows the absorption spectra when the excitations are from the lowest-energy SAC−CI states with A_2 symmetry, which have energies that are higher by 0.1−0.7 eV than the SAC A_1 ground state, depending on the h_{Pt} parameter. Clearly, in a metallic system such a population inversion is not possible. Here, our starting from a pure A_2 state merely serves as a

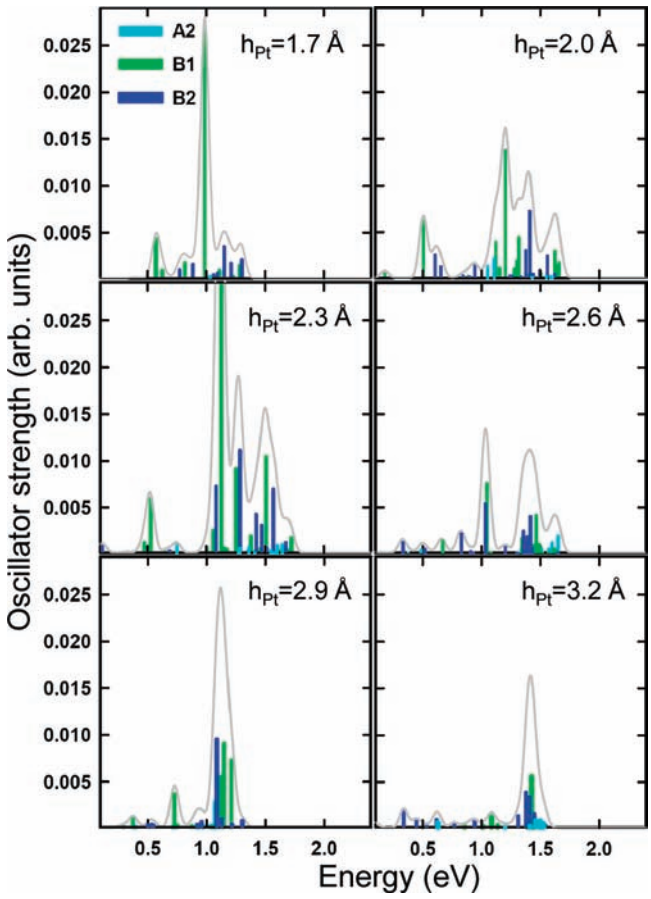

Figure 7. Excitation energies and the oscillator strengths (arbitrary units, same scale as in Figure 6) of the $(Pt_2)_2Cu_{74}$ structure for several values of the h_{Pt} parameter indicated in angstroms. The initial state of the excitation is the lowest-energy SAC−CI state with A_2 symmetry.

qualitative tool to identify peaks with respect to particular selection rules. In reality, the spectrum will be a temperature-dependent superposition of both spectra. In order to qualitatively calculate such optical spectra, one must take full account of the energetic redistribution of the electron population using the statistical operator $e^{-E_a/(k_BT)}$, where E_a is the energy of state a, k_B is the Boltzmann constant, and T is the temperature.[48] The transitions $A_2 \leftrightarrow A_1$ are forbidden by the selection rules, and compared to the previous situation, the intensity of the peaks are about 5 times smaller due to the small values of the transition dipoles. Similar to the previous case, the transitions oriented along the O_y axis (i.e., $A_2 \leftrightarrow B_1$) are the most prominent, while the smallest values of the oscillator strengths are due to the $A_2 \leftrightarrow A_2$ transitions which are oriented perpendicular to the Cu surface. For $h_{Pt} = 1.7$ Å, there are no peaks in the absorption spectrum in the 1.3−2 eV energy interval, contrary to the previous case when the transitions are from the SAC A_1 state.

An analysis of the SAC−CI coefficients allows one to identify the dominant single-particle transition corresponding to each excitation. For example, when the Pt dimers are close to the surface ($h_{Pt} = 1.7$ Å) and when the transitions are from the SAC A_1 state, the highest absorption peak corresponds to the excitation $A_1 \leftrightarrow B_2$ with energy 0.96 eV and oscillator strength 0.14. For this many-body excitation, the most dominant transition from occupied to empty MOs are the single excitations 504 → 509. For MO 504, the wave function is centered on the lower Cu atoms of the surface, with no contribution around the Pt adsorbates, while for MO 509 the wave function has an

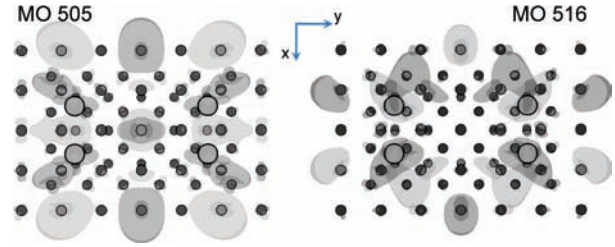

Figure 8. MO 505 (left) and MO 516 (right) of the $(Pt_2)_2Cu_{74}$ structure seen from above for $h_{Pt} = 1.7$ Å. The single-particle transition from the MO 505 to 516 is the dominant contribution to the $A_2 \leftrightarrow B_1$ excitation which gives the highest optical absorption peak at 0.98 eV (see the upper-left panel of Figure 7).

important contribution in the adsorbates region. This means that for this excitation charge is transferred from the surface toward the adsorbates. For the same geometry configuration, but when the excitation is from the A_2 state, the highest absorption peak occurs at 0.98 eV with intensity 0.026. In this case, the most dominant single-particle excitation is from MO 505 to 516. The shape of these MOs indicate that charge depletion occurs in the region between the Pt dimers at the end of the excitation, as can be seen from Figure 8. In the same manner, we are able to trace the origin of the excitation and to predict whether it corresponds to a transition from/to a MO that belongs to the adsorbates and the surface. Using all MOs in the active space might lead to a more rigorous computation of the excited sates, but a calculation with hundreds of MOs is intractable on the available state-of-the-art modern computers. Also, although a comparison with experiment is desirable, to date there is, at least to the best of our knowledge, no experimental data available for Pt dimers adsorbed on the Cu(001) surface.

Conclusions

We presented the soft landing of Pt dimers on Cu(001) using a large Cu cluster to model the surface. Clearly, by imposing the initial configuration and by fixing the symmetry, we are able to account for some of the many possible landing scenarios. Comparing the adsorption energies of the models we have studied, we found that the energetically most favorable case is when the Pt atoms of the dimers are situated above the hollow sites of the Cu lattice. A DOS analysis was carried out, showing how the presence of the substrate influences the electronic properties of the adsorbed clusters and vice versa. Comparing the DOS corresponding to the adsorption of one with the DOS of two Pt dimers on the Cu surface, as well as with the projected DOS of the separated subsystems, we were able to account for the surface-mediated interactions between the adsorbates. Optical absorption spectra were obtained using the excited states and the oscillator strengths calculated with the SAC−CI method, for various snapshots of soft landing. The positions and the widths of the absorption peaks change with the distance between the adsorbates and the substrate. We found that the most intense peaks of the absorption spectrum are around 1 eV and come from transitions from the SAC ground state to excited states with B_2 symmetry. Also, we computed symmetry-dependent spectra that may serve as unique signatures of the partial occupations of the lowest-energy states with A_1 and A_2 symmetry.

Acknowledgment. We would like to acknowledge the support from the Priority Programme 1153 of the German Research Foundation.

References and Notes

(1) Whitten, J. L.; Yang, H. *Surf. Sci. Rep.* **1996**, *24*, 55.
(2) Brivio, G. P.; Trioni, M. I. *Rev. Mod. Phys.* **1999**, *71*, 231.
(3) *Metal Clusters at Surfaces: Structure, Quantum Properties, Physical Chemistry*; Meiwes-Broer K. H., Eds.; Springer: Berlin, 2000.
(4) Kellogg, G. L.; Voter, A. F. *Phys. Rev. Lett.* **1991**, *67*, 622.
(5) Linderoth, T. R.; Horch, S.; Petersen, L.; Helveg, S.; Schønning, M.; Lægsgaard, E.; Stensgaard, I.; Besenbacher, F. *Phys. Rev. B* **2000**, *61*, 2448.
(6) Gurlu, O.; van Houselt, A.; Thijssen, W. H. A.; van Ruitenbeek, J. M.; Poelsema, B.; Zandvliet, H. J. W. *Nanotechnology* **2007**, *18*, 365305.
(7) te Velde, G.; Baerends, E. *J. Chem. Phys.* **1993**, *177*, 399.
(8) Wildberger, K.; Stepanyuk, V. S.; Lang, P.; Zeller, R.; Dederichs, P. H. *Phys. Rev. Lett.* **1995**, *75*, 509–512.
(9) Hammer, B.; Morikawa, Y.; Nørskov, J. K. *Phys. Rev. Lett.* **1996**, *76*, 2141.
(10) Pisani, C. *Phys. Rev. B* **1978**, *17*, 3143.
(11) Jakob, T.; Geschke, D.; Fritzsche, S.; Sepp, W.-D.; Fricke, B.; Anton, J.; Varga, S. *Surf. Sci.* **2001**, *486*, 194.
(12) Pacchioni, G. *Heterog. Chem. Rev.* **1995**, *2*, 213.
(13) Pavlyukh, Y.; Berakdar, J.; Hübner, W. *Phys. Rev. Lett.* **2008**, *100*, 116103.
(14) Lang, N.; Williams, A. *Phys. Rev. B* **1978**, *18*, 616.
(15) Messmer R. P. In *The Nature of the Surface Chemical Bond*; Rhodin, T. N., Ertl, G., Eds.; North-Holland: Amsterdam, 1979; p 51.
(16) Pettersson, L. G. M.; Faxen, T. *Theor. Chim. Acta* **1993**, *85*, 345.
(17) Panas, I.; Schüle, J.; Siegbahn, P.; Wahlgren, U. *Chem. Phys. Lett.* **1988**, *149*, 265.
(18) Panas, I.; Siegbahn, P. *J. Chem. Phys.* **1990**, *92*, 4625.
(19) Ackermann, L.; Rösch, N. *J. Chem. Phys.* **1994**, *100*, 6578.
(20) Strømsnes, H.; Jusuf, S.; Bagatur'yants, A.; Gropen, O.; Wahlgren, U. *Theor. Chim. Acta* **2001**, *106*, 329.
(21) Yudanov, I. V.; Sahnoun, R.; Neyman, K. M.; Rösch, N. *J. Chem. Phys.* **2002**, *117*, 9887.
(22) Yudanov, I. V.; Metzner, M.; Genest, A.; Rösch, N. *J. Phys. Chem. C* **2008**, *112*, 20269.
(23) Neyman, K. M.; Inntam, C.; Gordienko, A. B.; Yudanov, I. V.; Rösch, N. *J. Chem. Phys.* **2005**, *122*, 174705.
(24) Hermann, K.; Bagus, P. S.; Nelin, C. J. *Phys. Rev. B* **1987**, *35*, 9467.
(25) C. W. Bauschlicher, J. *J. Chem. Phys.* **1994**, *101*, 3250.
(26) van Daelen, M. A.; Li, Y. S.; Newsam, J. M.; van Santen, R. A. *J. Phys. Chem.* **1996**, *100*, 2279.
(27) Reddy, B. V.; Pederson, M. R.; Khanna, S. N. *Phys. Rev. B* **1997**, *55*, R7414.
(28) Lewis, S. P.; Rappe, A. M. *J. Chem. Phys.* **1999**, *110*, 4619.
(29) Sudhyadhoma, A.; Micha, D. A. *J. Chem. Phys.* **2006**, *124*, 101102.
(30) Frisch, M. J.; Trucks, G. W.; Schlegel, H. B.; Scuseria, G. E.; Robb, M. A.; Cheeseman, J. R.; Montgomery, J. A.; Jr.; Vreven, T.; Kudin, K. N.; Burant, J. C.; Millam, J. M.; Iyengar, S. S.; Tomasi, J.; Barone, V.; Mennucci, B.; Cossi, M.; Scalmani, G.; Rega, N.; Petersson, G. A.; Nakatsuji, H.; Hada, M.; Ehara, M.; Toyota, K.; Fukuda, R.; Hasegawa, J.; Ishida, M.; Nakajima, T.; Honda, Y.; Kitao, O.; Nakai, H.; Klene, M.; Li, X.; Knox, J. E.; Hratchian, H. P.; Cross, J. B.; Bakken, V.; Adamo, C.; Jaramillo, J.; Gomperts, R.; Stratmann, R. E.; Yazyev, O.; Austin, A. J.; Cammi, R.; Pomelli, C.; Ochterski, J. W.; Ayala, P. Y.; Morokuma, K.; Voth, G. A.; Salvador, P. J.; Dannenberg, J.; Zakrzewski, V. G.; Dapprich, S.; Daniels, A. D.; Strain, M. C.; Farkas, O.; Malick, D. K.; Rabuck, A. D.; Raghavachari, K.; Foresman, J. B.; Ortiz, J. V.; Cui, Q.; Baboul, A. G.; Clifford, S.; Cioslowski, J.; Stefanov, B. B.; Liu, G.; Liashenko, A.; Piskorz, P.; Komaromi, I.; Martin, R. L.; Fox, D. J.; Keith, T.; Al-Laham, M. A.; Peng, C. Y.; Nanayakkara, A.; Challacombe, M.; Gill, P. M. W.; Johnson, B.; Chen, W.; Wong, M. W.; Gonzalez, C.; Pople, J. A. *Gaussian 03, Revision D.01*, Gaussian, Inc., Wallingford CT, 2004.
(31) Becke, A. D. *Phys. Rev. A* **1988**, *38*, 3098.
(32) Lee, C.; Yang, W.; Parr, R. G. *Phys. Rev. B* **1988**, *37*, 785.
(33) Hey, P. J.; Wadt, W. R. *J. Chem. Phys.* **1985**, *82*, 299.
(34) Hurley, M. M.; Pacios, L. F.; Christiansen, P. A.; Ross, R. B.; Ermler, W. C. *J. Chem. Phys.* **1986**, *84*, 6840.
(35) Graham, A. P.; Hofmann, F.; Toennies, J. P.; Chen, L. Y.; Ying, S. C. *Phys. Rev. Lett.* **1997**, *78*, 3900.
(36) Braun, O. M.; Valkering, T. P.; van Opheusden, J. H.; Zandvliet, H. *Surf. Sci.* **1997**, *384*, 129.
(37) Tomatsu, K.; Nakatsuji, K.; Iimori, T.; Takagi, Y. H.; Kusuhara, A. I.; Komori, F. *Science* **2007**, *315*, 1696.
(38) Montalenti, F.; Ferrando, R. *Surf. Sci.* **1999**, *432*, 27.
(39) Wulfhekel, W.; Hattink, B. J.; Zandvliet, H. J. W.; Rosenfeld, G.; Poelsema, B. *Phys. Rev. Lett.* **1997**, *79*, 2494.
(40) Mo, Y. *Science* **1993**, *261*, 886.
(41) Sudhyadhom, A.; Micha, D. A. *J. Chem. Phys.* **2006**, *124*, 101102.
(42) Grönbeck, H.; Andreoni, W. *Chem. Phys.* **2000**, *262*, 1.
(43) Pavlyukh, Y.; Hübner, W. *Eur. Phys. J. D* **2002**, *21*, 239.
(44) The value of 2.34 Å between the Pt atoms of a free dimer is in excellent agreement with the experimental value; see. Gupta, S. K; Nappi, B. M.; Gingerich, K. A. *Inorg. Chem.* **1981**, *20*, 966.
(45) Nakatsuji, H.; Hirao, K. *J. Chem. Phys.* **1978**, *68*, 2053.
(46) Nakatsuji, H. *Chem. Phys. Lett.* **1979**, *67*, 329.
(47) Nakatsuji, H. *Chem. Phys. Lett.* **1979**, *67*, 334.
(48) Lefkidis, G.; Hübner, W. *Phys. Rev. B* **2006**, *74*, 155106.

JP904133B